doi:10.1111/evo.14210

Polygenic local adaptation in metapopulations: A stochastic eco-evolutionary model

Enikő Szép,[1,*] Himani Sachdeva,[1,2,*] and Nicholas H. Barton[1,3]

[1] *Institute of Science and Technology Austria, Am Campus 1, Klosterneuburg 3400, Austria*

[2] *Department of Mathematics, University of Vienna, Vienna 1090, Austria*

[3] *E-mail: nick.barton@ist.ac.at*

Received June 20, 2020
Accepted February 13, 2021

This article analyzes the conditions for local adaptation in a metapopulation with infinitely many islands under a model of hard selection, where population size depends on local fitness. Each island belongs to one of two distinct ecological niches or habitats. Fitness is influenced by an additive trait which is under habitat-dependent directional selection. Our analysis is based on the diffusion approximation and accounts for both genetic drift and demographic stochasticity. By neglecting linkage disequilibria, it yields the joint distribution of allele frequencies and population size on each island. We find that under hard selection, the conditions for local adaptation in a rare habitat are more restrictive for more polygenic traits: even moderate migration load per locus at very many loci is sufficient for population sizes to decline. This further reduces the efficacy of selection at individual loci due to increased drift and because smaller populations are more prone to swamping due to migration, causing a positive feedback between increasing maladaptation and declining population sizes. Our analysis also highlights the importance of demographic stochasticity, which exacerbates the decline in numbers of maladapted populations, leading to population collapse in the rare habitat at significantly lower migration than predicted by deterministic arguments.

KEY WORDS: **Demographic stochasticity, eco-evolutionary dynamics, extinction, local adaptation, metapopulation, polygenic selection.**

Adaptation to environmental change is often rapid (Thompson 1998; Kinnison and Hendry 2001; Grant and Grant 2006; Kokko and López-Sepulcre 2007) and time scales of ecological and evolutionary change comparable, giving a feedback between demography and evolution. Fisher (1930) first described reciprocal interactions between population size and adaptation, leading to the notion of hard selection, whereby high genetic load drives populations to extinction. This is an extreme example of a more general feedback: an increase in genetic load due to deleterious variants reduces population size; smaller populations are affected more strongly by drift and gene flow, which increase the fixation of locally deleterious alleles, further decreasing size.

Such eco-evolutionary feedbacks are crucial during evolutionary rescue following a sudden environmental shift (Gomulkiewicz and Holt 1995; Gonzalez et al. 2013), and are key to the survival of marginal populations (Kawecki 2008), the colonization of peripheral habitats (Barton and Etheridge 2018; Sachdeva 2019), and the emergence of sharp range margins in the absence of environmental discontinuities (Polechová and Barton 2015; Polechová 2018).

Eco-evolutionary feedbacks are especially important in fragmented habitats, where stochastic extinction and recolonization of patches require recurrent bouts of rapid adaptation, especially if selective pressures vary across patches. This type of metapopulation structure may arise, for instance, if multiple hosts are available within the same region (Carroll and Boyd 1992; Dobler and Farrell 1999), favoring host-specific adaptations. The potential for local adaptation and the stability of subpopulations then depends on the interaction between selection (which is mediated by

[*] Joint first authors.

the genetic architecture of selected traits), dispersal (which protects populations from inbreeding load and stochastic extinction, but may also introduce maladapted phenotypes), and demography (which is affected by mean genetic fitness, and in turn influences the efficacy of selection).

Previous theory on the persistence of subdivided populations neglects key aspects of this interplay. For instance, Blanquart et al. (2012) analyze conditions for local adaptation in a spatially heterogeneous metapopulation under *soft* selection (i.e., constant population sizes), thus neglecting the feedback between fitness and demography. Ronce and Kirkpatrick (2001) explicitly model the effects of maladaptation on population sizes in a metapopulation with multiple ecologically distinct habitats but neglect all stochasticity. Another approach, exemplified by Hanski and Mononen (2011), considers re-colonization of patches to be instantaneous and extinction to depend deterministically on patch fitness. However, this fails to address how the coupled *stochastic* dynamics of genotype frequencies and population sizes influence extinction thresholds. Conversely, almost all work on stochastic fluctuations in metapopulations neglects natural selection (Lande 1993; Lande et al. 1998; Ovaskainen and Meerson 2010).

A better understanding of the link between maladaptation and extinction also requires genetically realistic eco-evolutionary models. However, at present, most metapopulation models assume one of two extreme architectures (Lion 2018; Govaert et al. 2019): either mutations occur one by one (adaptive dynamics), or there are very many infinitesimal-effect loci (quantitative genetics). While the latter can describe response from standing variation (which often underlies rapid adaptation), with a few exceptions (Ronce and Kirkpatrick 2001; Hanski and Mononen 2011), quantitative genetic models only deal with migration into a *single* population (e.g., Tufto 2001; Chevin et al. 2017; Barton and Etheridge 2018).

Here, we investigate the joint evolution of population size and allele frequencies in a metapopulation consisting of infinitely many islands connected via migration. Each island belongs to one of two different habitats characterized by distinct selection pressures. We ask: when are demographically stable, locally adapted populations maintained within islands belonging to the "rare" or marginal habitat? Conversely, when does maladaptive gene flow from the abundant habitat reduce the rare habitat to a maladapted (and possibly nearly extinct) sink? Understanding evolution in marginal habitats has important implications for range limits and the long-term survival of metapopulations; moreover, local adaptation in marginal habitats may be the first step towards speciation.

A key focus of our work is on how the coupling between population size and mean fitness (hard selection) influences local adaptation and extinctions. Such coupling places severe constraints on the survival and adaptation of interconnected populations: gene flow limits local adaptation not only by overwhelming selection at individual loci but also through the effect of migration load on population size. Segregation of locally maladaptive alleles at many loci at even low frequencies substantially reduces mean fitness, causing lower population numbers, which further impairs selection at individual loci, resulting in a positive feedback between population decline and loss of local adaptation ("migrational meltdown"; see Ronce and Kirkpatrick 2001).

As we demonstrate next, random fluctuations in population size (demographic stochasticity) as well as in allele frequencies (genetic drift) strongly influence thresholds for maladaptation and extinction. Thus, going beyond deterministic analyses by considering both sources of stochasticity within a common framework is crucial for understanding extinction: smaller populations are more prone to fix maladaptive alleles due to genetic drift and swamping from larger populations; this further reduces the fitness and size of small populations, rendering them even more vulnerable to demographic fluctuations and chance extinction, even in parameter regimes where demographic stochasticity *by itself* (i.e., in the absence of maladaptation) is of little consequence.

A second focus is to understand how the feedback between population size and fitness is mediated by the genetic basis of selected traits. In particular, is maladaptation (and possibly extinction) in the rare habitat more or less likely for more polygenic traits? Understanding polygenic local adaptation within subdivided populations is challenging due to statistical associations, that is, linkage disequilibria (LD) between loci. Our theoretical analysis neglects such associations, assuming linkage equilibrium (LE) within demes, and becomes exact in the limit where all processes are much slower than recombination. Thus, LE allows us to work solely with allele frequencies. However, LE does *not* imply that loci evolve independently: under hard selection, evolutionary dynamics of different loci become coupled through their aggregate effects on population size, which in turn influences individual loci via genetic drift.

Our analysis is based on a *diffusion approximation* for the joint stochastic evolution of allele frequencies and population size. The diffusion approximation has been widely used in population genetics (Fisher 1922; Kimura 1955) but remains less prominent in ecology, and has only been used to model stochastic population dynamics, without genetics (e.g., Lande 1993; Mangel and Tier 1993). Our framework incorporates both demographic stochasticity and genetic drift, following Banglawala (2010). The full model requires numerical solution, but explicit analytical predictions are possible in various biologically interesting limits. In order to assess the importance of LE and other assumptions, we compare theoretical predictions against individual-based simulations with a finite number of demes.

Model and Methods

Consider a metapopulation with infinitely many islands (demes) that exchange genes via a common pool. We assume that any island belongs to one of two local habitats, indexed by $\alpha = 1, 2$. A fraction $1 - \rho$ (or ρ) of islands belong to the first (or second) habitat. We choose $\rho < 1/2$, such that ρ always denotes the fraction in the rare habitat, indexed as habitat 2 hereafter.

Individuals are haploid and express an additive trait influenced by L unlinked, biallelic loci with alternative states denoted by $X = 0, 1$. The trait is assumed to be under directional selection toward one or the other extreme: thus, a genotype with all "1" alleles or all "0" alleles has maximum fitness in the first or second habitat, respectively. For simplicity, the maximum possible genetic fitness in either habitat is assumed to be the same. Thus, individual fitness is given by $\exp[-\sum_{j=1}^{L} s_{1,j}(1 - X_j)]$ and $\exp[-\sum_{j=1}^{L} s_{2,j}X_j]$ in the two habitats, where $s_{1,j} > 0$ (or $s_{2,j} > 0$) denotes the strength of selection against the locally disfavored allele at locus j in habitat 1 (or 2), and X_j the allelic state at locus j.

The life cycle of individuals consists of dispersal, followed by selection and mating. As our focus is on how gene flow influences selected polymorphisms, we neglect other sources of variation. However, the framework easily extends to include mutation. In each generation, individuals migrate with probability m into a common pool; migrants from this pool are then evenly redistributed over islands. The assumption of infinitely many islands means that genotype frequencies in the migrant pool are essentially deterministic; in simulations, we model a large but finite number of islands.

We assume hard selection, where population sizes are stochastic but influenced by mean fitness on the island plus local density-dependent regulation: the size n_i^* on island i, after selection and regulation, is a Poisson random variable with mean $n_i \overline{W}_i e^{r_{0,i}(1-n_i/K_i)}$. Here, $r_{0,i} \geq 0$ is the baseline rate of growth, K_i the baseline carrying capacity, n_i the population size prior to selection, and $\overline{W}_i$ the mean genetic fitness on island i. For simplicity, we assume $r_{0,i} = r_0$ and $K_i = K$ across all islands. The n_i^* offspring are formed by randomly sampling $2n_i^*$ parents (with replacement) from the n_i individuals in proportion to individual fitness, and then creating offspring via free recombination of each pair of parent genotypes. Note that selection is density independent, that is, relative fitness of genotypes is independent of population size.

When selection is strong relative to migration and drift, and the number of loci not very large, populations can adapt to their local habitat, resulting in LD between alleles favored within a habitat. Our theoretical framework, however, assumes that selection per locus and migration are weak compared to recombination, such that LD within a deme (generated by immigration of individuals from differently adapted habitats) is rapidly dissipated and can be neglected. This allows us to consider the coupled dynamics of population size and L alleles (rather than 2^L genotypes) while still accounting for stochastic effects via the diffusion approximation.

For weak growth, selection and migration (i.e., $r_0, s, m \ll 1$), we can use a continuous time approximation for allele frequency and population size dynamics. The size n_i and the allele frequency $p_{i,j}$ at the jth locus on the ith island satisfy the following *coupled* equations (see also Supporting Information Appendix A1 for details):

$$\frac{\partial n_i}{\partial t} = \left[r_0\left(1 - \frac{n_i}{K}\right) + r_{g,i}\right]n_i + m(\overline{n} - n_i) + \lambda_{n_i}(t) \qquad (1a)$$

$$\frac{\partial p_{i,j}}{\partial t} = p_{i,j}(1 - p_{i,j})\frac{\partial r_{g,i}}{\partial p_{i,j}} + m\frac{\overline{n}}{n_i}\left[\frac{\overline{np}_j}{\overline{n}} - p_{i,j}\right] + \lambda_{p_{i,j}}(t). \qquad (1b)$$

Here, $r_{g,i}$ is the genetic component of the growth rate (i.e., the log fitness) averaged over all genotypes on island i. For the fitness functions described above, we have: $r_{g,i} = -\sum_{j=1}^{L} s_{1,j}q_{i,j}$ for an island in the first habitat and $-\sum_{j=1}^{L} s_{2,j}p_{2,j}$ in the second habitat. Here $p_{i,j}$ and $q_{i,j} = 1 - p_{i,j}$ denote the frequencies of the "1" and "0" alleles at locus j on island i.

Note that the dynamics of any one deme are coupled to the dynamics of all other demes via the mean number of immigrants $m\overline{n}$ and the mean number of immigrant alleles $m\overline{np_j}$ (at locus j) per unit time (where $\overline{n}$ is the population size and $\overline{np_j}$ the number of allele copies per deme, averaged over the metapopulation).

Equation (1a) describes how population size evolves over time on an island in a given habitat. The first term within the square brackets describes logistic growth, and the second describes how growth rates are reduced relative to the baseline r_0 due to habitat-dependent selection against locally disfavored alleles; this term $r_{g,i}$ couples population sizes to allele frequencies. The second term describes migration, which makes a net positive contribution when the focal deme is smaller than the average $\overline{n}$ across the metapopulation. The third term $\lambda_{n_i}(t)$ is an uncorrelated random process with $\mathbb{E}[\lambda_{n_i}] = 0$ and $\mathbb{E}[\lambda_{n_i}(t)\lambda_{n_i}(t')] = n_i(t)\delta(t - t')$, where $\mathbb{E}[\ldots]$ denotes an average over independent realizations. This describes fluctuations of population size due to demographic stochasticity, inherent in reproduction and death. Since the number of offspring is Poisson distributed, the variance of population sizes is just $n_i(t)$. Note that the noise term can generate local extinctions even in well-adapted populations: extinction arises from the stochastic dynamics, rather than being imposed arbitrarily.

Equation (1b) describes allele frequency dynamics at locus j: the first term corresponds to selection against the locally deleterious allele; the second term describes the effect of migration, which pulls allele frequencies towards the metapopulation

average ($\overline{np}_j/\overline{n}$), which is the allele frequency in the migrant pool. Islands with larger populations contribute more to the migrant pool; they are also less prone to swamping by maladaptive alleles because the migration term in equation (1b) is inversely proportional to n_i. This results in a positive feedback: better adapted islands are more populous, send out more migrants and are less affected by incoming, maladapted individuals, maintaining local adaptation more easily. Fluctuations in allele frequencies are described by $\lambda_{p_{i,j}}(t)$, which satisfies $\mathbb{E}[\lambda_{p_{i,j}}] = 0$ and $\mathbb{E}[\lambda_{p_{i,j}}(t)\lambda_{p_{i,j}}(t')] = [(p_{i,j}(t)q_{i,j}(t))/n_i(t)]\delta(t-t')$ (where $q(t) = 1 - p(t)$), as in the haploid Wright-Fisher model.

Equations (1a) and (1b) can be made dimensionless by rescaling population size to the carrying capacity K, and all evolutionary rates to the baseline growth rate r_0. This gives the following rescaled parameters (denoted by uppercase letters): $T = r_0 t,\ M = m/r_0,\ S = s/r_0,\ N = n/K$, and the new parameter $\zeta = r_0 K$, which represents the number of births per unit time at carrying capacity, and hence governs the magnitude of demographic fluctuations. Both scaled and unscaled parameters are tabulated in Table 1.

DIFFUSION APPROXIMATION FOR THE JOINT DISTRIBUTION OF ALLELE FREQUENCIES AND POPULATION SIZE

The time evolution of the joint probability distribution $\Psi_i(N, p_1, \ldots, p_L)$ of allele frequencies $\{p_1, \ldots, p_L\}$ and (rescaled) population size N on any island in habitat i is described by the diffusion approximation, which depends only on the mean and variance of the change in N and $\{p\}$ per unit time. For ease of notation, the vector $(N, p_1, \ldots p_L)$ is denoted by $\mathbf{x}$. We have

$$\begin{aligned}\frac{\partial}{\partial\tau}\Psi_i(\mathbf{x},\tau) = &-\frac{\partial}{\partial N}\left[A_N^{(i)}(\mathbf{x})\Psi_i(\mathbf{x})\right] + \frac{1}{2\zeta}\frac{\partial^2}{\partial N^2}[B_N(\mathbf{x})\Psi_i(\mathbf{x})] \\ &-\sum_{j=1}^{L}\frac{\partial}{\partial p_j}\left[A_{p_j}^{(i)}(\mathbf{x})\Psi_i(\mathbf{x})\right] \\ &+\frac{1}{2\zeta} \\ &\sum_{j=1}^{L}\frac{\partial^2}{\partial p_j^2}\left[B_{p_j}(\mathbf{x})\Psi_i(\mathbf{x})\right] \qquad (2)\end{aligned}$$

$$A_N^{(i)}(\mathbf{x}) = [1 - N + R_{g,i}]N + M(\bar{N} - N)$$

$$A_{p_j}^{(i)}(\mathbf{x}) = p_j(1-p_j)\frac{\partial R_{g,i}}{\partial p_j} + M\frac{\bar{N}}{N}\left[\frac{\overline{Np_j}}{\bar{N}} - p_j\right]$$

$$B_N(\mathbf{x}) = N \qquad B_{p_j}(\mathbf{x}) = \frac{p_j(1-p_j)}{N}.$$

The equation is expressed in terms of rescaled parameters and $\zeta = r_0 K$ (see above). Here, $A_N^{(i)}$ and $A_{p_j}^{(i)}$ specify the expected rate of change of the population size and allele frequencies on an island in habitat i (see also eq. 1), and B_N and B_{p_j} the

Table 1. Key notation.

ρ	Fraction of islands in the rare habitat; fraction in the common habitat is $1-\rho$ (where $\rho < 1/2$)
$r_{0,i}$	Baseline growth rate on island i; $r_{0,i} = r_0$ for all i
K_i	Baseline carrying capacity of island i; $K_i = K$ for all i
L	Number of loci influencing the additive trait
$s_{i,j}$	Coefficient of selection against the locally disfavored allele at locus j in habitat i
m	Fraction of individuals that migrate
n_i	Population size on island i
$p_{i,j}$	Frequency (of the "1" allele) at locus j on island i; $q_{i,j} = 1 - p_{i,j}$
$r_{g,i}$	Genetic component of growth rate (i.e., log fitness) averaged over all genotypes on island i; given by $-\sum_{j=1}^{L} s_{i,j}q_{i,j}$ and $-\sum_{j=1}^{L} s_{i,j}p_{i,j}$ for islands in first and second habitats, respectively
$\bar{n}$, $\overline{np_j}$	Mean population size and mean number of "1" alleles at locus j per deme, averaged over all islands
$\mathbb{E}_i(n)$, $\mathbb{E}_i(np_j)$	Expected population size and expected number of "1" alleles at locus j for a deme in habitat i, obtained by integrating over the equilibrium joint distribution for population size and allele frequencies
Scaled parameters	
$N = n/K$	Population size scaled by carrying capacity
$S = s/r_0, M = m/r_0$	Selection coefficient, migration rate scaled by intrinsic growth rate
$\zeta = r_0 K$	Average number of births per unit time at carrying capacity; the strength of demographic fluctuations is inversely proportional to ζ

variance of the change per unit time (which is independent of habitat). The dependence on the local habitat arises only through the average log fitness $R_{g,i} = r_{g,i}/r_0$, given by $-\sum_{j=1}^{L} S_{1,j}q_j$ and $-\sum_{j=1}^{L} S_{2,j}p_j$ in the first and second habitats, respectively.

In principle, equation (2) can be numerically integrated to obtain the joint distribution of N and $\{p_j\}$ through time. However, we focus on the stationary (equilibrium) distribution. This depends on the numbers and genetic composition of the migrant pool, which is determined by the average number of individuals $\overline{N}$ and allele copies $\{\overline{Np_j}\}$ (for each locus) across the metapopulation. The stationary distribution on any island in habitat i is given by (see Supporting Information Appendix A2 for details):

$$\Psi_i(N, \{p_j\}|\overline{N}, \{\overline{Np_j}\}) = \frac{1}{Z} N^{2\zeta M\overline{N}-1} \mathrm{e}^{-\zeta[(1-M)-N]^2} \mathrm{e}^{2\zeta N R_{g,i}} \prod_{j=1}^{L} p_j^{2\zeta M\overline{Np}_j - 1}(1-p_j)^{2\zeta M(\overline{N}-\overline{Np}_j)-1}, \quad (3)$$

where Z is the normalization constant.

NUMERICAL SOLUTION FOR THE EQUILIBRIUM

The state of each deme is determined by the average number of immigrant individuals $m\overline{N}$ and of immigrant alleles $m\{\overline{Np_j}\}$ (at each locus j) per unit time. Given these, we can find the expected numbers and allele frequencies $\{\mathbb{E}_i[N], \mathbb{E}_i[Np_j]\}$ on an island within habitat i, by integrating over the stationary distribution (eq. 3). Here, the expectations $\mathbb{E}[\ ]$ can be thought of as averages for a *given* island, obtained by averaging over replicate metapopulations (or simulations) or over uncorrelated timepoints at equilibrium within a single simulation. The crucial point is that at equilibrium, the average across all demes in the metapopulation at any instant (denoted by $\overline{\ }$) must equal the weighted sum of expected values across habitats (Rouhani and Barton 1993). Thus,

$$\overline{N} = (1-\rho)\mathbb{E}_1[N] + \rho\mathbb{E}_2[N],$$
$$\overline{Np_j} = (1-\rho)\mathbb{E}_1[Np_j] + \rho\mathbb{E}_2[Np_j]. \quad (4)$$

Equilibria are located by starting at an arbitrary $\{\overline{N}, \overline{Np_j}\}$, calculating $\{\mathbb{E}_i[N], \mathbb{E}_i[Np_j]\}$ using equation (3), then computing the new $\{\overline{N}, \overline{Np_j}\}$ using equation (4), and iterating until a fixed point. With this procedure, either a polymorphism is found, or one or other allele is fixed. In principle, this procedure simultaneously yields the equilibrium population size and allele frequencies at all the L loci (which may have different effect sizes and hence attain different frequencies). However, iterating over an $L+1$-dimensional space is computationally intensive. We thus restrict attention to the case with effect sizes equal at all loci, such that $S_{1,j} = S_1$ and $S_{2,j} = S_2$ for all j. Then, we need to find only the fixed point $\{\overline{N}, \overline{Np}\}$.

In principle, populations may evolve toward different equilibria depending on their initial state. However, we find that outcomes are largely insensitive to initial frequencies (unless these are very extreme) except when migration rates are close to the threshold for loss of polymorphism and $LS \gtrsim 1$. Here, we will show the equilibrium that is attained starting with maximal genetic variation in each population (allele frequency 0.5 at each locus).

The above procedure for finding equilibria is exact, given the diffusion approximation which, however, relies on three assumptions. First, we assume all processes to be sufficiently slow ($r_0, m, s \ll 1$) that a continuous time approximation (eq. 1) is valid. Second, we assume infinitely many demes, such that mean population size and allele frequency over the metapopulation exhibit negligible fluctuations, even though within any one deme, they follow a distribution (eq. 3). This allows us to treat the migrant pool as deterministic, and completely characterized by $\overline{N}$ and $\overline{Np_j}$. Finally, we assume that demes are in LE, that is, LD between locally adaptive alleles at different loci is negligible. This final assumption is justified when recombination is much faster than other processes, that is, as the unscaled parameters s, m, $r_0 \to 0$. We investigate the sensitivity of our results to each of these assumptions using individual-based simulations in the Supporting Information (Appendix C), but focus on the most critical assumption, namely that of LE, in the main text.

As the full model involves several parameters, and calculating the joint distribution requires a numerical solution for $\overline{N}$ and $\overline{Np}$, it is useful to consider some simpler limits. We first consider population dynamics in the absence of selection ($S_1 = S_2 = 0$), and examine how demographic stochasticity and migration affect metapopulation survival. We then introduce selection, but assume that it is weak relative to the baseline growth rate, that is, $Ls_i \ll r_0$ or $LS_i \ll 1$; we also neglect demographic stochasticity. In this "soft selection" limit, population sizes are decoupled from fitnesses and both well-adapted and maladapted demes are at carrying capacity.

We then consider scenarios where selection against maladapted genotypes is strong enough to affect population dynamics, that is, $LS_1, LS_2 \sim 1$ (for equal-effect loci) resulting in "hard selection," wherein less fit populations are smaller and may even go extinct. We examine hard selection using the equilibrium distribution $\psi(N, p_1, \ldots p_L)$ derived above, as well as a simpler "semideterministic" approximation that accounts for genetic drift but neglects demographic stochasticity, and treats population sizes as depending deterministically on mean fitnesses. In the main article, we focus on symmetric selection across habitats ($S_1 = S_2 = S$); $S_1 \neq S_2$ is considered in Supporting Information Appendix B.

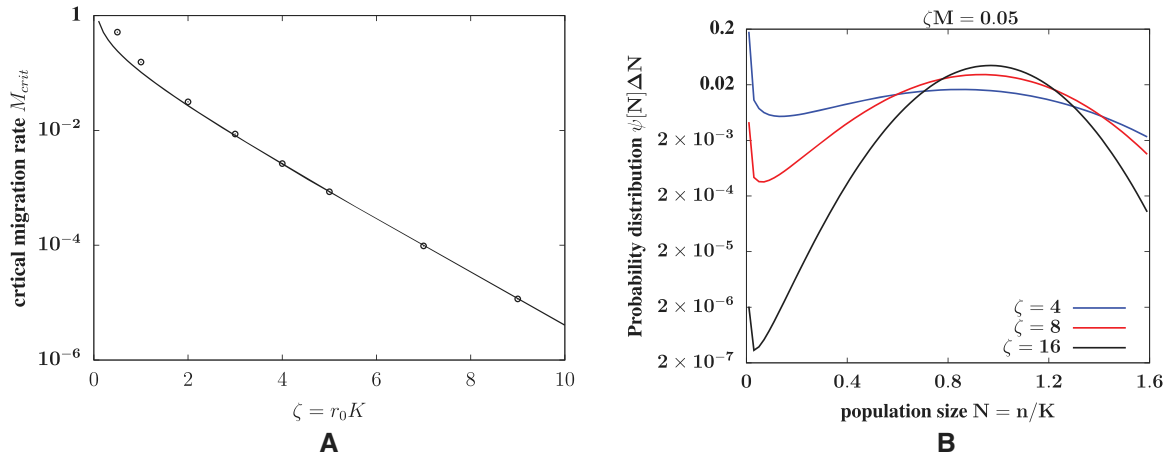

Figure 1. Deme sizes in the purely demographic model with no selection. (A) The migration threshold M_{crit}, below which the entire metapopulation goes extinct due to demographic fluctuations, versus $\zeta = r_0 K$. The threshold M_{crit} falls exponentially with increasing ζ. Points show results of the diffusion approximation; the solid line depicts the large ζ approximation: $M_{crit} \approx e^{-\zeta}/(2\sqrt{\pi\zeta})$. (B) Probability distribution $\psi[N]$ of the scaled population size $N = n/K$ (integrated over intervals of width $\Delta N = 0.02$), obtained from the diffusion approximation, for various ζ, for $\zeta M = 0.05$. The migration rate M is reduced as ζ is increased, to keep $2\zeta M = Km$ fixed. The fraction of nearly extinct demes falls with increasing ζ. Diffusion approximation predictions are obtained from eq. S5 of the Supporting Information.

Results

EFFECT OF DEMOGRAPHIC STOCHASTICITY AND MIGRATION IN THE ABSENCE OF SELECTION

Consider a scenario with no selection, such that population sizes are independent of allele frequencies, and only affected by demographic fluctuations and migration. Although individual demes fluctuate, $\overline{N}$ over the metapopulation evolves deterministically. Demes are coupled through $\overline{N}$, which determines the expected number of immigrants per deme. Using equation (3), we can derive the distribution $\psi[N|\overline{N}]$ of population sizes N, conditioned on $\overline{N}$ (Supporting Information Appendix A3). The expected population size, $\mathbb{E}(N|\overline{N})$ in any deme, given $\overline{N}$, is obtained by integrating over $\psi[N|\overline{N}]$, and then equating $\mathbb{E}(N|\overline{N}) = \overline{N}$. This yields one or more equilibria for $\overline{N}$.

There is always an equilibrium at $\mathbb{E}(N) = \overline{N} = 0$, which corresponds to extinction of the whole metapopulation. Above a critical migration rate M_{crit}, there may also be an equilibrium with $\overline{N} > 0$. This M_{crit} is the migration rate at which the equilibrium $\overline{N} = 0$ becomes unstable (Supporting Information Appendix A3). Figure 1A shows that the M_{crit} required for metapopulation survival decreases exponentially: $M_{crit} \approx e^{-\zeta}/(2\sqrt{\pi\zeta})$ as $\zeta = r_0 K$ increases.

Above this migration threshold, the metapopulation survives as a whole; however, individual islands undergo extinctions and recolonizations if the average number of immigrants is small, that is, for $2\zeta M\overline{N} = 2m\overline{n} < 1$, which corresponds to $2\zeta M \lesssim 1 + \frac{1}{2\zeta} + \cdots$ (Supporting Information Appendix A3). In this case, the distribution of N is bimodal (Fig. 1B): a fraction of demes is near extinction, whilst the remainder have population sizes normally distributed around $N = 1 - M$ (i.e., $n = K(1 - m/r_0)$), with variance $1/2\zeta = 1/(2r_0 K)$. The fraction of nearly extinct demes falls with increasing ζ, for a given $2\zeta M$ (Fig. 1B). For migration rates that are still higher ($2\zeta M \gg 1$), individual demes never go extinct and exhibit essentially deterministic dynamics.

The parameter $\zeta = r_0 K$ thus governs the extent of demographic stochasticity: it determines the threshold for global extinction (Fig. 1A), the probability of local extinctions (Fig. 1B), as well as the variance of population numbers around carrying capacity (among occupied demes). Henceforth, we consider growth rates and carrying capacities that are sufficiently high (i.e., $\zeta = r_0 K \gg 1$) that local extinctions in the *absence* of maladaptation are exceedingly unlikely. However, even for $\zeta \gg 1$, maladapted populations may be affected by demographic stochasticity and become extinct.

SOFT SELECTION (CONSTANT POPULATION SIZE)

We next introduce selection, but assume that the evolutionary change it effects is slow compared to population growth (i.e., $LS \ll 1$), and that $\zeta = r_0 K \gg 1$ (as above). Then the model reduces to the classical infinite island model with soft selection (Wright 1932), where population sizes are fixed at carrying capacity ($n = K$) on each island. Unlike in the case with hard selection, allele frequencies at different loci evolve independently under soft selection (assuming LE) because genetic drift at any

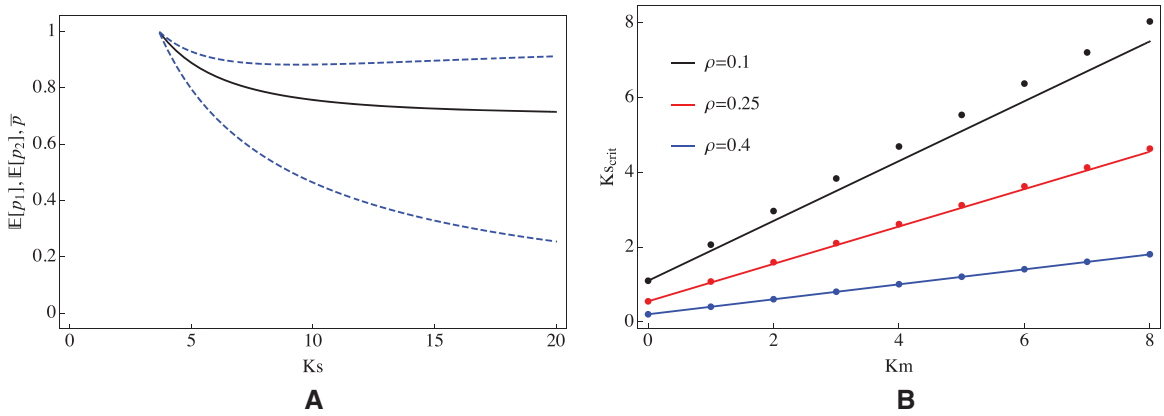

Figure 2. **Local adaptation under soft selection. (A) Expected allele frequencies in the two habitats (dashed), and the overall mean over the metapopulation (solid), versus Ks, as obtained from the diffusion. The fraction of demes in the rare habitat is $\rho = 0.3$, the average number of migrants per generation is $Km = 8$; selection is symmetric: $s_1 = s_2 = s$. (B) The critical selection coefficient Ks_c, above which a polymorphic equilibrium with $0 < \overline{p} < 1$ can be maintained, as a function of Km, the average number of migrants exchanged between demes, for various ρ. Points show the diffusion prediction; lines show the approximation $Ks_c = \frac{1}{2}\log(\frac{1-\rho}{\rho}) + Km(1-2\rho)$. Allele frequencies under soft selection are obtained from the diffusion approximation by using equation (S6) in the Supporting Information.**

locus just depends on a fixed population size, and not on adaptation at other loci. Thus, we need only consider the allele frequency distribution $\psi[p]$ at one locus: this was first derived by Wright (1932), and also emerges from the joint distribution in equation (3) (Supporting Information Appendix A4). This is also the basis of Blanquart et al.'s (2012) single-locus analysis.

The expected allele frequency $\mathbb{E}(p|\overline{p})$ in a deme, given the mean $\overline{p}$ in the migrant pool, is obtained by integrating over $\psi[p]$ (Supporting Information Appendix A4). Allele frequencies in different demes are coupled via the mean allele frequency, $\overline{p}$, among migrants: within any deme, migration pulls the expected allele frequency toward $\overline{p}$, whereas selection drives $\mathbb{E}_1[p]$ toward 1 (or $\mathbb{E}_2[p]$ toward 0). Since all demes have equal sizes, they contribute equally to the migrant pool. Thus at equilibrium, we have $\overline{p} = (1-\rho)\mathbb{E}_1(p|\overline{p}) + \rho\mathbb{E}_2(p|\overline{p})$, which allows us to numerically find the equilibrium allele frequency in each habitat and across the metapopulation (Fig. 2A).

There are always equilibria corresponding to $\overline{p} = 1$ or $\overline{p} = 0$ (i.e., when the whole metapopulation is fixed for one or other allele). A polymorphic equilibrium (with $0 < \overline{p} < 1$) can be maintained when selection exceeds a threshold s_c (Fig. 2A), such that alleles favored in the rare habitat can invade. As selection becomes stronger, the different habitats approach fixation for different alleles. Thus, both habitats may be simultaneously adapted only if $s > s_c$. For $s < s_c$, alleles that confer a selective advantage in the common habitat fix across the entire metapopulation. Interestingly, the critical selection strength s_c approaches a nonzero value as $m \to 0$ (Fig. 2B) as long as one habitat is rarer than the other. Thus, this bias toward alleles favored in the common habitat persists even in the limit of very low migration, for which we would have (erroneously) expected allele frequencies in different demes to evolve independently.

To understand the dependence of s_c on m, it is useful to first consider a purely deterministic analysis, which ignores genetic drift (and thus requires Ks, $Km \gg 1$). This predicts that polymorphism can only be maintained above a critical selection coefficient $s_c = m(1-2\rho)$ (Supporting Information Appendix A4), where ρ is the fraction of demes in the rare habitat. However, as $s \to s_c$, we expect $\overline{q} \to 0$ and thus $Km\overline{q} \to 0$ (Fig. 2A). In other words, irrespective of how large Km is, near the threshold for loss of polymorphism, the numbers of alleles (of the rarer type) entering any deme will be very low and subject to random fluctuations due to drift. Thus the deterministic prediction only provides a lower bound on the true s_c, as drift will further erode polymorphism.

In the opposite limit of low migration ($Km \to 0$), loci will be near fixation for one or other allele, making it necessary to account for drift. The rates of fixation toward and away from an allele with advantage s, at frequency $\overline{p}$ in the migrant pool, are in the ratio $\sim (\overline{p}/\overline{q})e^{2Ks}$, such that the expected frequency of the favored allele in the deme is $\overline{p}e^{2Ks}/(\overline{p}e^{2Ks} + \overline{q})$ (Supporting Information Appendix A4). Thus, with $s_1 = s_2 = s$, the metapopulation reaches an equilibrium at

$$\overline{p} = (1-\rho)\frac{\overline{p}e^{2Ks}}{\overline{p}e^{2Ks} + \overline{q}} + \rho\frac{\overline{p}}{\overline{p} + \overline{q}e^{2Ks}}. \quad (5)$$

A polymorphic equilibrium at $\overline{p} = \frac{(1-\rho)e^{2Ks} - \rho}{e^{2Ks} - 1}$ becomes possible if $Ks > Ks_c$ where $Ks_c = \frac{1}{2}\log(\frac{1-\rho}{\rho})$ (in the $Km \to 0$ limit). Thus, even in the limit of very low migration, selection must exceed a critical threshold to prevent swamping of locally favored

alleles in the rare habitat. Note that this effect is not captured by the deterministic analysis above (which erroneously predicts $s_c \to 0$ as $m \to 0$).

Numerically computing the equilibrium allele frequency, we find that the threshold s_c increases linearly with m (points in Fig. 2B). This is approximated by: $Ks_c \approx \frac{1}{2}\log(\frac{1-\rho}{\rho}) + Km(1-2\rho)$ (solid lines in Fig. 2B), where the first term is the $Km \to 0$ prediction (which accounts for drift) and the second term the corresponding deterministic prediction (which neglects drift).

HARD SELECTION

When net selection against maladapted phenotypes is comparable to the baseline growth rate, that is, $Ls \sim r_0$ or $LS \sim 1$ (assuming L equal-effect loci), changes in mean fitness have a substantial effect on population size, and maladapted populations are prone to extinction. Selection at *individual* loci need not be strong: typical effect sizes may be small enough (i.e., $\zeta S = Ks \leq 1$) that drift can degrade adaptation at individual loci. However, if the number of loci L affecting fitness is large, selection, in aggregate, is strong. If local adaptation is to be possible even in large populations, then migration must be weak relative to selection per locus, that is, $M(1-2\rho) < S$. Further, we assume $\zeta = r_0 K \gg 1$, so that local extinctions in the absence of maladaptation are highly improbable.

In the following, we use the joint distribution (eq. 3) to identify the conditions under which locally adapted, stable populations are maintained in both habitats. We first analyze two examples in detail to illustrate the qualitatively different outcomes under weak vs. strong coupling (feedback) between population size and mean fitness (Fig. 3). We also compare theoretical predictions (which assume LE) with the results of individual-based simulations for these two examples, to clarify when LD can be neglected and the diffusion approximation becomes accurate (Fig. 4). We then explore more generally how critical migration (or selection) thresholds for local adaptation depend on demographic stochasticity, the number of selected loci, and the fraction of the rare habitat.

Figure 3 shows how polygenic adaptation collapses within the rare habitat as migration increases above a critical value in a scenario with weak coupling between population size and mean fitness, that is, $LS < 1$ (Fig. 3A and B) and in a strong coupling, that is, $LS > 1$ scenario (Fig. 3C and D). Figure 3 shows theoretical predictions for the expected allele frequencies and population sizes in the two habitats, as well as the distribution of population sizes in the rare habitat (insets). Figure 4 compares theoretical predictions with results of individual-based simulations.

In both strong and weak coupling scenarios, alternative alleles are close to fixation in either habitat at low migration. As M increases, the frequency of the locally favored allele (Fig. 3A and D) and the expected population size N (Fig. 3B and D) decline in both habitats due to increasing migration load. At a critical migration rate M_c, the rarer allele is lost, the population in the rare habitat crashes, and the overall $\overline{N}$ falls to a minimum. For $LS > 1$, the loss of local adaptation results in near extinction of the (maladapted) deme, while with weak coupling ($LS < 1$), completely maladapted demes survive at a finite fraction of carrying capacity.

As M increases beyond M_c, populations in the rare habitat increase marginally, signifying that this habitat is now a maladapted demographic sink. The emergence of source-sink dynamics at high M causes numbers in the common habitat to decline slightly with M. This is outweighed by the faster increase in numbers in the rare habitat, resulting in a slight increase in overall $\overline{N}$ at large M. There is another migration threshold below which the whole metapopulation collapses because colonization is too rare (Fig. 1A); however, this threshold is negligibly small ($\sim e^{-\zeta}/(2\sqrt{\pi\zeta})$) for large ζ (here, $\zeta = 40$), and is not visible here.

Figure 3B and D also depicts how the distribution $\psi[N]$ of the (scaled) population size in the rare habitat changes across the threshold M_c (insets). With weak coupling ($LS < 1$), population sizes are approximately normally distributed about a nonzero expected value $\mathbb{E}[N]$ irrespective of local adaptation, that is, for both $M < M_c$ and $M > M_c$ (inset, Fig. 3B). Further, $\mathbb{E}[N] \sim 1 - LS\mathbb{E}[p]$, where $\mathbb{E}[p]$ is the expected allele frequency of the locally deleterious allele in the rare habitat. By contrast, with strong coupling (i.e., $LS > 1$), the distribution is bimodal for $M \leq M_c$ (i.e., when the rare habitat is locally adapted): a small fraction of demes is nearly extinct and the remaining have numbers that are approximately normally distributed around $\mathbb{E}[N] \sim 1 - LS\mathbb{E}[p]$. The fraction of nearly extinct demes in the rare habitat increases on approaching M_c (solid vs. dashed distribution, inset Fig. 3D). Above the threshold M_c, the distribution collapses to a single peak at $N = 0$ (i.e., all demes are nearly extinct) and decays exponentially with N. The threshold for loss of local adaptation is sharper for larger LS—a finding that we clarify next.

The theoretical results shown in Figure 3 are based on the joint distribution of population size and allele frequencies (eq. 3), derived by neglecting LD. As discussed above, we expect LD to be negligible and our analytical predictions to hold exactly in the limit where recombination is much faster than all other processes. This corresponds to taking the limit $s, m, r_0 \to 0$, $K \to \infty$, while holding the *scaled* parameters $S = s/r_0$, $M = m/r_0$ and $\zeta = r_0 K$ fixed.

To test this expectation, we compare theoretical predictions for the expected allele frequency in the rare habitat with individual-based simulations where the unscaled parameters r_0, s and m are progressively reduced and the carrying capacity K increased, while holding fixed the scaled parameters $\zeta = r_0 K$, $S = s/r_0$, and $M = m/r_0$ (note that the equilibrium is fully determined by scaled parameters under LE). These comparisons

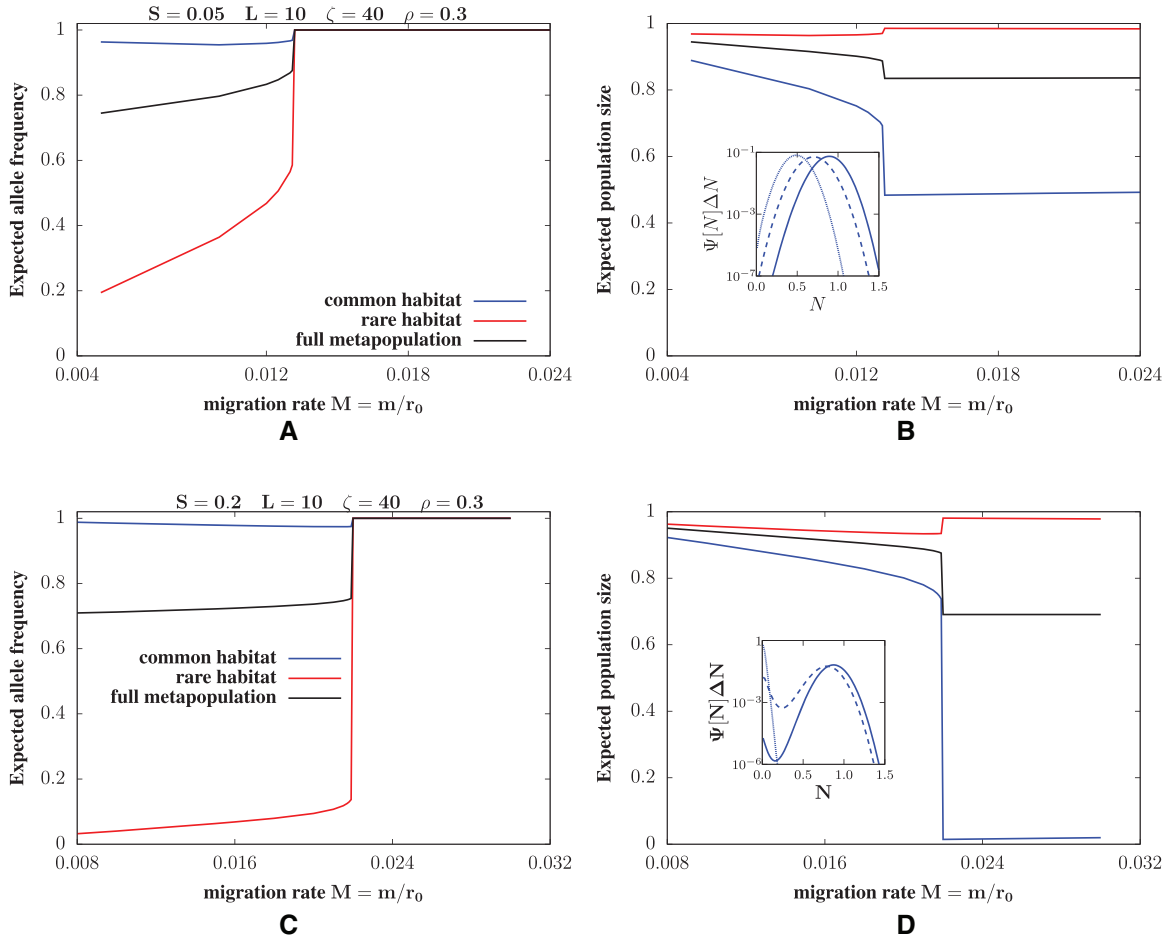

Figure 3. Loss of local adaptation at a critical migration rate under hard selection. Expected allele frequencies of the "1" allele (left panels), which is favored in the common habitat and disfavored in the rare habitat, and expected population sizes (right panels) versus scaled migration rate $M = m/r_0$, for (A)–(B) weak coupling ($S = 0.05$, $LS = 0.5$) and (C)–(D) strong coupling ($S = 0.2$, $LS = 2$) between population size and mean fitness. The number of selected loci is $L = 10$ and selection is symmetric, with $S_1 = S_2 = S = s/r_0$ at each locus; the rare habitat comprises 30% of demes ($\rho = 0.3$) and $\zeta = r_0K = 40$. The plots show the expected allele frequencies and sizes in the rare and common habitat (blue, red) as well as the mean $\overline{p}$ and $\overline{N}$ across the whole metapopulation (black). For both weak coupling (i.e., $LS < 1$ in (A) and (B)) and strong (i.e., $LS > 1$ in (C) and (D)), there is a critical migration threshold, M_c, above which alleles favored in the rare habitat are lost from the metapopulation. The insets in (B) and (D) depict the probability distribution $\psi[N]$ of population sizes in the rare habitat (integrated over intervals of width $\Delta N = 0.02$) for $M < M_c$ (solid line, corresponding to $M = 0.005$ in B and $M = 0.014$ in D), $M \sim M_c$ (dashed line, corresponding to $M = 0.013$ in B and $M = 0.0219$ in D), and $M > M_c$ (dotted line, corresponding to $M = 0.021$ in B and $M = 0.03$ in D). For weak coupling, $\psi[N]$ peaks at a nonzero N, irrespective of M. For strong coupling, $\psi[N]$ is bimodal for $M \lesssim M_c$, with one peak close to $N = 0$ (corresponding to nearly extinct demes) and the other peak at $N \sim 1 - LS\mathbb{E}[p]$ (corresponding to a well-adapted demes). For $M > M_c$, the second peak disappears and the distribution is concentrated at $N = 0$ (all demes nearly extinct). All plots are obtained from the diffusion approximation by numerically determining fixed points (eqs. 3 and 4) using the joint distribution $\Psi[N, p]$.

(Fig. 4) show that the migration threshold for loss of local adaptation in simulations can be significantly higher than the theoretical M_c if LS is high (Fig. 4B). High values of LS correspond to high values of Ls, which governs the extent to which the *effective* migration rate of a deleterious allele is reduced due to its genetic background, when the two habitats are nearly fixed for alternative alleles at multiple loci (see also Supporting Information Appendix C). However, as expected, the critical migration threshold in simulations converges to the theoretical prediction (for a given set of scaled parameters ζ, S, M) as evolutionary and ecological processes become weaker (r_0, s, $m \to 0$) relative to recombination. Note that for $LS < 1$ (Fig. 4A), the allele frequencies in individual-based simulations are very close to the theoretical (LE) prediction for all r_0, suggesting that LD is already negligible even for the highest value of r_0 (red). The minor discrepancy between simulations and theory in this case is due to the relatively few demes in the simulation, and vanishes as we simulate metapopulations with more demes (results not shown).

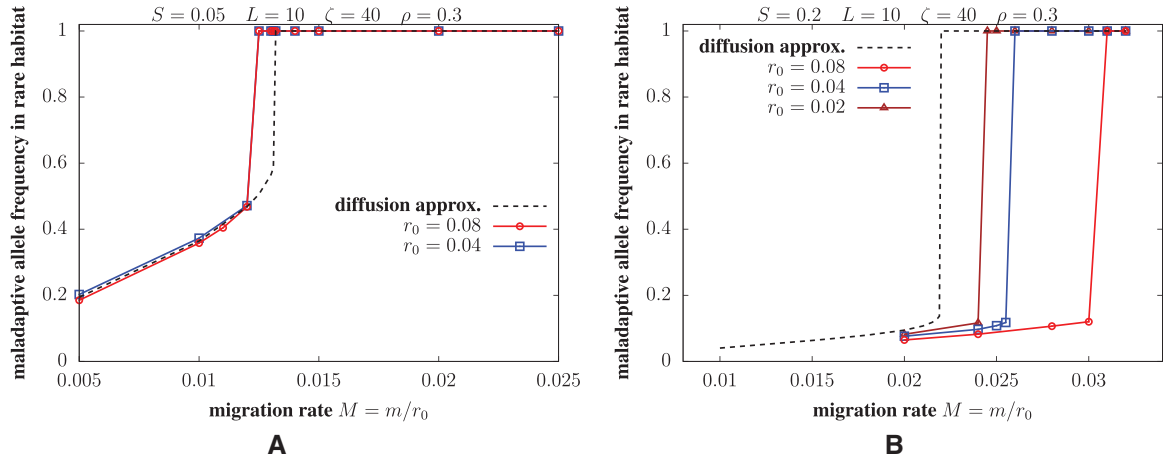

Figure 4. Comparison of the predictions of the diffusion approximation (which assumes LE) with individual-based simulations (which incorporate LD). Expected allele frequencies of the locally disfavored allele in the rare habitat versus scaled migration rate $M = m/r_0$, for (A) weak coupling ($S = 0.05$, $LS = 0.5$) and (B) strong coupling ($S = 0.2$, $LS = 2$) between population size and mean fitness. All parameters are the same as in Figure 3. In each plot, the different colors show results of individual-based simulations (of 100 islands) for different values of r_0. All other unscaled parameters s, m, K are varied (as described in the text) as we vary r_0, such that the scaled parameters $S = s/r_0$, $M = m/r_0$ and $\zeta = r_0K$ are the *same* for the different colors. The results of individual-based simulations deviate significantly from the diffusion prediction which assumes LE (dashed line) for larger r_0, especially for $LS > 1$ (panel B), but converge toward the LE prediction as we approach smaller r_0 while holding scaled parameters fixed. We only simulate 2 values of r_0 in panel A, as deviations from the LE prediction are already small even with the highest value of r_0.

In the following, we will only present theoretical predictions obtained from equations (3) and (4) (which assume LE), with the understanding that these will accurately describe evolutionary outcomes in the well-defined limit in which LD is negligible.

SEMIDETERMINISTIC APPROXIMATION

The fact that population sizes are approximately normally distributed about $\mathbb{E}(N)$ for $LS \leq 1$, suggests that in this "weak coupling" regime, we can use a simpler approximation by neglecting fluctuations in N and assuming that, at any instant, it is close to its expected value $\mathbb{E}(N)$, which depends deterministically on the expected fitness $\mathbb{E}[R_g]$ through $\mathbb{E}(N) \approx 1 + \mathbb{E}[R_g]$. This *semideterministic* approximation (details in Supporting Information Appendix A5) thus accounts for how allele frequencies within any deme are influenced by genetic drift (whose strength is inversely proportional to the local population size N), but assumes that N itself is largely unaffected by demographic fluctuations and determined by the expected allele frequencies (through $\mathbb{E}[R_g]$). This approximation is thus only meaningful if $\zeta \gg 1$, so that demographic fluctuations in *well-adapted* populations are weak. As shown next, the semideterministic approximation accurately predicts the threshold for loss of local adaptation if $LS \leq 1$ (i.e., when the distribution of N is unimodal about the expected population size).

In this regime (i.e., when the semideterministic approximation is accurate), outcomes are governed by three parameters. For a given ρ (i.e., fraction of demes in the rare habitat), and assuming symmetric selection $S_1 = S_2 = S$, these are: $\zeta S = Ks$, which governs the strength of drift relative to selection in a population at carrying capacity, $\zeta M = Km$, which determines the average number of migrants exchanged between demes at carrying capacity, and LS, which determines how much population sizes are reduced below carrying capacity due to maladaptation (see also Supporting Information Appendix A5). Next, we clarify the roles of these parameters in the low migration limit $\zeta M = Km \ll 1$, which is most conducive to local adaptation, and then build upon this to understand the more complex scenario where gene flow impairs adaptation more strongly.

LOW MIGRATION LIMIT

Under rare migration, loci are near fixation for one or other allele within a deme. As with soft selection, this implies that the fixation rates of alternative alleles (at a given locus) on island i are in the ratio $\approx (\overline{Np}/\overline{N})e^{2\zeta S_i N_i} : 1 - (\overline{Np}/\overline{N})$, where $\zeta = r_0K$, and S_i is the (scaled) selective advantage of the locally favored allele at that locus on island i. Further, $\overline{Np}/\overline{N}$ is the frequency (within the migrant pool) of alleles favored on island i. A comparison of this heuristic (for fixation rates) under hard selection with the analogous approximation under soft selection (eq. 5) highlights two important features of allele frequency evolution under hard selection.

First, the rate of fixation and hence the frequency of the favored allele at any locus within any deme depends on the degree of maladaptation at all other loci via the local population size N_i.

In particular, locally deleterious alleles at very many loci, at even modest frequencies, can have substantial effects (in aggregate) on mean fitness, thus reducing size. This further accentuates drift at individual loci, causing locally deleterious alleles to increase or even fix, further reducing population size, thus generating a positive feedback between loss of fitness and decline in numbers.

Second, any island contributes to the allele frequency $\overline{Np}/\overline{N}$ in the migrant pool in proportion to its size, which depends on the fitness of the island. Since locally adaptive alleles are at slightly lower frequency in the rare as opposed to the common habitat (even when both are locally adapted), demes are also somewhat smaller in the rare habitat. Thus, demes in the rare habitat contribute less to the allele frequency in the migrant pool than demes within the common habitat in proportion to the ratio of population sizes. This causes the allele frequency in the migrant pool to shift further toward the optimum for the common habitat, which increases migration load and reduces numbers in the rare habitat, generating a second positive feedback loop. Crucially, both types of feedback depend on the strength of coupling between population size and mean fitness, and are thus stronger for larger $LS = L(s/r_0)$.

Figure 5A shows how local adaptation depends on the selective advantage of the favored allele per locus $S = s/r_0$ or alternatively, the number of selected loci L, for a *fixed* LS under very weak migration ($\zeta M = 0.005$). These plots thus reveal how local adaptation is influenced by the genetic architecture of (i.e., the number and selective effects of loci contributing to) genetic load, for a given total load LS, which translates into a given maximum possible reduction in population size under hard selection.

Figure 5A shows that given a certain maximum load LS, local adaptation in the rare habitat is possible only above a critical S_c per locus. For $S < S_c$, drift overpowers selection at individual loci, causing alleles favored in the common habitat to eventually fix across the entire metapopulation, despite very low genetic exchange, as with soft selection (Fig. 2B). Alternatively, given a certain (maximum) load LS, local adaptation is possible only if the selected trait is determined by a modest number of loci (i.e., for $L < L_c$, where $L_c = L(S/S_c)$), and fails for highly polygenic traits.

Further, local adaptation in the rare habitat requires stronger selection per locus when the total cost of maladaptation, LS, is higher (solid vs. dashed lines in Fig. 5A). In fact, the critical selection threshold S_c increases with increasing number of loci under divergent selection, such that local adaptation is not possible for *any* S for sufficiently large L even under weak migration (Fig. 5B). As we argue next, higher S increases the efficacy of selection at individual loci (via ζS) but also results in stronger reduction in population size N due to load (via LS): the latter effect is especially strong for more polygenic traits, so that an increase in S may actually result in weaker selection relative to drift.

Thus, as selection becomes less "hard," that is, $LS = L(s/r_0)$ becomes smaller with $\zeta S = Ks$ and $Km = \zeta M$ held fixed, allele frequencies in the two habitats should approach those under soft selection. This is indeed what we see (Fig. 5C): for a given ζS, the frequency of the locally favored allele under hard selection *increases* towards the soft selection prediction as we approach lower S (and hence lower LS). Note that keeping ζS fixed corresponds to increasing carrying capacities as selection is reduced, such that the strength of selection relative to drift remains unchanged even as it becomes weaker relative to population growth.

Finally, S_c is lower for larger ρ (orange vs. blue plots in Fig. 5A), that is, if the rare habitat encompasses a larger fraction (but still less than half) of the islands. In this case, the rare habitat is subject to a lower migration load (because allele frequencies in the migrant pool are more intermediate), resulting in a weaker reduction in population size as well as weaker swamping at individual loci.

We now ask: for a given $\zeta M = Km$, does local adaptation depend only on the composite parameters $\zeta S = Ks$ and LS, as one would expect under a semideterministic regime? To investigate this, we determine the threshold ζ_c (such that local adaptation occurs for $\zeta > \zeta_c$), as a function of S, for various L and fixed ζM. Here, ζM is held constant by reducing the rescaled migration rate $M = m/r_0$ as $\zeta = r_0 K$ increases, such that the average number of migrants (between demes at carrying capacity) remains unchanged.

Figure 5D shows that the semideterministic prediction for $\zeta_c S$ (dashed line, obtained from eq. S7 of the Supporting Information) is extremely accurate for $LS \lesssim 1$: in this regime, the threshold $\zeta_c S$ for local adaptation in the rare habitat depends on the number of selected loci only via the combination LS (which governs the reduction in population size due to maladaptation). Moreover, this threshold only increases sublinearly with LS for $LS \lesssim 1$. By contrast, for $LS \gtrsim 1$, the semideterministic approximation fails: the critical $\zeta_c S$ threshold increases much faster (nearly linearly) with LS than predicted by the semideterministic approximation. However, even in this regime, the threshold for adaptation $\zeta_c S$ depends only weakly on the number of loci, and is essentially governed by LS.

Note that the semideterministic approximation significantly underpredicts $\zeta_c S$ (i.e., the extent to which selection per locus must prevail over drift) for large LS (Fig. 5D). For $LS > 1$, individual demes within the habitat may be maladapted and nearly extinct, even when the rare habitat is adapted as a whole. Thus, the distribution of population sizes is intrinsically bimodal (Fig. 3D) and poorly approximated by a single population size (as assumed by the semideterministic approximation). Moreover demographic stochasticity may be important at low population numbers, even if it has negligible effects near carrying capacity (i.e., if $\zeta = r_0 K \gg 1$). Thus, accounting for the full *stochastic*

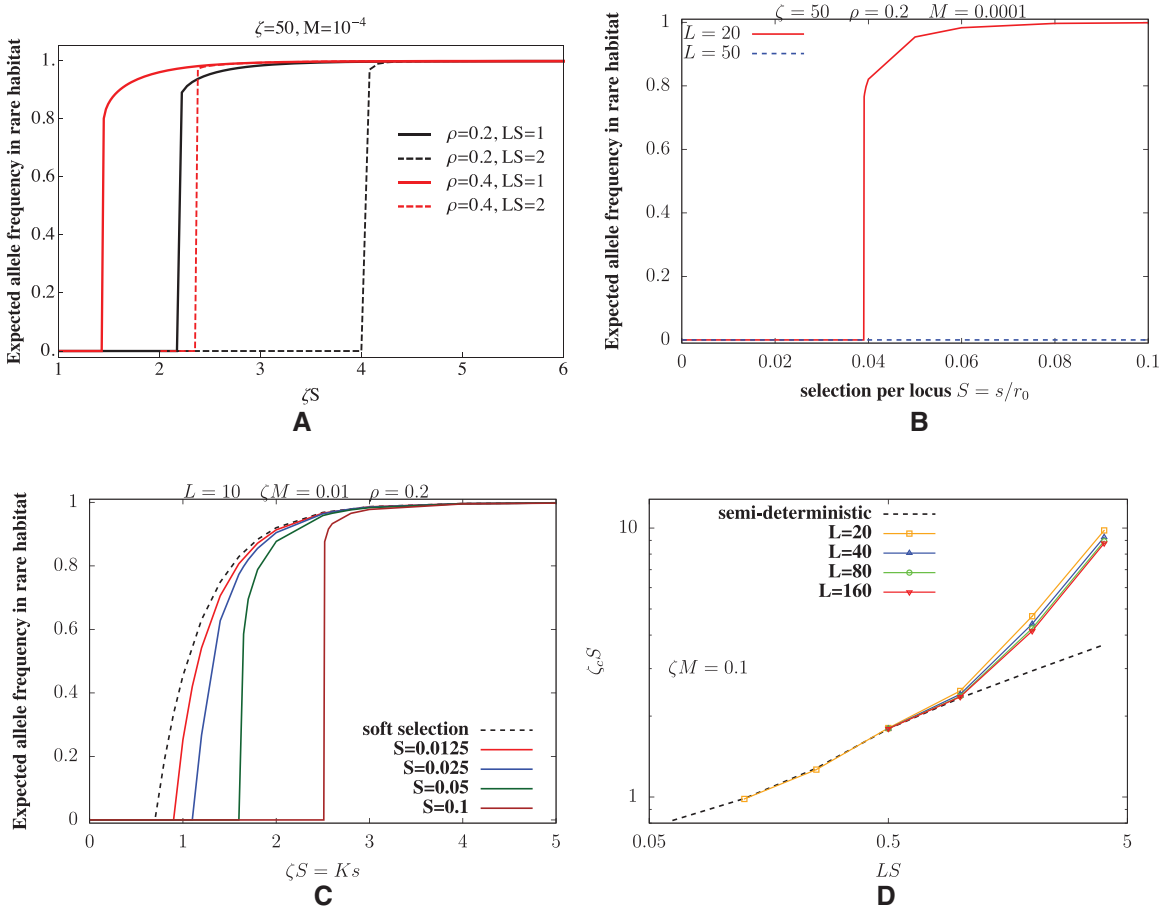

Figure 5. Local adaptation in the rare habitat under hard selection with weak migration ($\zeta M = Km \ll 1$); selection is symmetric across the two habitats ($S_1 = S_2 = S = s/r_0$). (A and B) Expected frequency of the locally favored allele in the rare habitat vs. $\zeta S = Ks$, for $\zeta = r_0 K = 50$, $M = 0.0001$ for (A) fixed LS (B) fixed L (and $\rho = 0.2$). (A) As we move along the x-axis, the scaled selection coefficient S and the number of loci L are changed simultaneously such that maximum possible genetic load LS is constant (for any one curve). Solid versus dashed lines correspond to $LS = 1$ and $LS = 2$, respectively. Different colors correspond to different fractions ρ of demes in the rare habitat. Local adaptation in the rare habitat is lost when selective architectures are highly polygenic with weak selective effect per locus (high L, low S). (B) Local adaptation in the rare habitat is not possible at any selection strength S, for larger L (blue), which depends on ζ. (C) Expected frequency of the locally favored allele in the rare habitat versus $\zeta S = Ks$ for different $S = s/r_0$, for $\zeta M = Km = 0.01$, $\rho = 0.2$, and $L = 10$. For a given S, the composite parameter $\zeta S = Ks$ is varied by varying ζ; M is changed accordingly so that ζM is constant. The dashed line shows the corresponding prediction for allele frequencies as a function of Ks when population sizes are fixed, that is, decoupled from fitness (soft selection). For a given $\zeta S = Ks$, populations approach the soft selection prediction as S and hence LS (which determines the coupling between population size and fitness) decrease. (D) Comparison of the predictions of the full stochastic model for the critical selection threshold $\zeta_c S$ against the semideterministic prediction (which neglects demographic fluctuations and treats population size on each island as being determined by the local expected fitness). The threshold $\zeta_c S$ for local adaptation in the rare habitat is plotted against LS for different values of L (depicted by different symbols), for $\zeta M = 0.1$ and $\rho = 0.2$. For given L, we vary LS by changing S, and then compute the critical ζ_c for each S. The migration rate M is changed accordingly such that ζM is constant at 0.1. The symbols and solid lines represent predictions of the full stochastic model while the dashed line represents predictions of the semideterministic approximation. There is good quantitative agreement between the full model and the semideterministic approximation for $LS \lesssim 1$, but not for larger LS. Predictions of the full stochastic model with hard selection are obtained by determining fixed points numerically (eqs. 3 and 4) using the joint distribution $\Psi[N, p]$; the soft selection prediction (dashed line in (C)) is obtained by determining fixed points under soft selection (eq. S6 in Supporting Information); the semideterministic prediction (dashed line in (D)) is obtained by determining fixed points of the semideterministic equations (eq. S7 in Supporting Information).

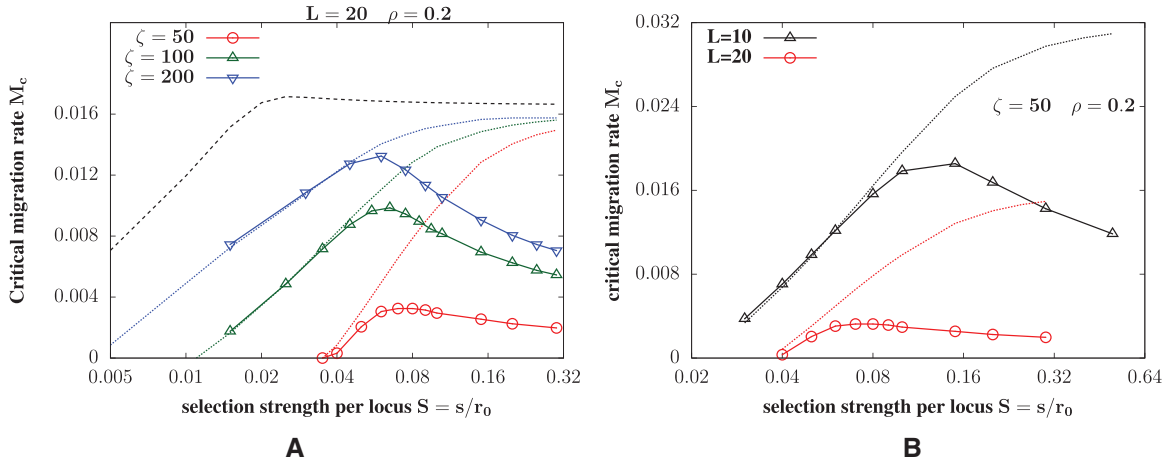

Figure 6. Critical migration rates for loss of local adaptation in the rare habitat. Critical (scaled) migration rate $M_c = m_c/r_0$ versus (scaled) selection coefficient $S = s/r_0$ per locus for (A) different values of ζ for $L = 20$, (B) different values of L for $\zeta = 50$, with $S_1 = S_2 = S$ and $\rho = 0.2$ in both cases. Symbols with solid lines depict M_c obtained from the joint stochastic distribution of population size and allele frequencies; dotted lines represent the predictions of the semideterministic approximation (obtained from eq. S7 of the Supporting Information); dashed line in (B) represents the deterministic prediction. M_c falls with S for large S: this effect is not captured by the semideterministic or the deterministic prediction. For any S, the critical migration rate M_c increases with increasing ζ (in panel A).

distribution of population sizes and allele frequencies is crucial for predicting evolutionary outcomes in this regime.

CRITICAL MIGRATION RATES FOR LOSS OF LOCAL ADAPTATION IN THE RARE HABITAT

Where selection is strong relative to drift (for a given LS), so that both habitats are locally adapted under low genetic exchange, we ask: how high can migration be while still allowing adaptation to the rare habitat and polymorphism overall? Figure 6 shows M_c, the critical migration rate above which polymorphism collapses, as a function of S for symmetric selection ($S_1 = S_2 = S$), for different values of ζ with L fixed (Fig. 6A) or different values of L with ζ fixed (Fig. 6B). The points represent results of the full stochastic model (based on the joint distribution of N and p); dotted lines show predictions of the semideterministic approximation (which neglects demographic stochasticity); the dashed line in Figure 6A shows the fully deterministic prediction (which neglects both demographic stochasticity and drift).

It is useful to first consider the deterministic (dashed lines in Fig. 6A) and semideterministic (dotted lines) predictions for the critical migration rate M_c: both analyses predict that M_c should increase with S when selection is weak but then saturate to a constant value for large S. The semideterministic prediction for M_c is lower than the deterministic prediction due to the contribution of drift to maladaptation but approaches the deterministic prediction as ζ (and hence ζS) increase. The emergence of a selection-independent threshold M_c at large S (under the deterministic analysis) is most easily demonstrated in the $\rho \to 0$ limit, in which one of the habitats is extremely rare and does not affect allele frequencies in the other habitat. In this simple limit, we can show that $M_c \sim 1/(4L)$ for $L \gg 1$ and large S (Supporting Information Appendix A6). More generally, this reflects the fact that under hard selection, a population is viable only while its total migration load is less than its intrinsic growth rate r_0. Since genetic load per locus is *at least* m in the limit of a very rare habitat ($\rho \to 0$), and is typically greater than m under hard selection (Supporting Information Appendix A6), this limits how many polymorphic loci can be maintained without extinction.

Now, consider the predictions of the fully stochastic analysis (symbols in Fig. 6A), which accounts for both drift and demographic stochasticity. When selection is weak, the critical migration rate M_c increases with S and is accurately predicted by the semideterministic analysis. However, beyond a certain threshold selection strength, which corresponds approximately to $LS \sim 1$ (Fig. 6B), M_c *declines* with increasing S. Thus, the range of migration rates allowing local adaptation in the rare habitat is widest (i.e., M_c largest), for intermediate selection. As expected, M_c decreases with increasing L (in accordance with the difficulty of maintaining polygenic local adaptation under hard selection) and increases with increasing ζ (where higher $\zeta = r_0 K$ implies weaker stochastic fluctuations in both population sizes and allele frequencies). However, even for ζ as high as 200 (i.e., 200 births per generation in a well-adapted population), M_c is much lower than the corresponding deterministic threshold for large LS (Fig. 6A).

The nonmonotonic dependence of M_c on selection per locus appears quite generally, that is, for various ζ (Fig. 6A), L (Fig. 6B) and ρ (results not shown), and is in sharp contrast to

expectations under soft selection (where M_c is predicted to increase linearly with S), or to predictions for hard selection that fail to account for the stochastic distribution of population sizes (dashed and dotted lines in Fig. 6). More specifically, loss of local adaptation in the large LS regime is accompanied by an increase in the fraction of nearly extinct demes; demographic stochasticity further exacerbates extinction risk in populations that may be already shrinking due to maladaptive gene flow, thus causing M_c to be several times lower than the deterministic prediction.

Discussion

Existing theory on maladaptation and extinction in metapopulations is largely based on simple genetic models and fails to address the stochastic coevolution of population sizes and allele frequencies. While various models include one or other stochastic process, for example, genetic drift in subdivided populations (Whitlock and Barton 1997; Blanquart et al. 2012), stochastic extinction-recolonization dynamics in metapopulations (Hanski and Mononen 2011), demographic and environmental fluctuations in the absence of selection (Mangel and Tier 1993; Lande et al. 2003; Black and McKane 2012), very few model the combined effects of different types of stochasticity (though see Chevin et al. 2017).

Our modeling framework is based on a diffusion approximation for the joint evolution of population sizes and allele frequencies under hard selection (Banglawala 2010; Barton and Etheridge 2018), which we extend here to a metapopulation with multiple ecological niches. It assumes a polygenic architecture for local adaptation, and accounts for both genetic drift and demographic stochasticity. It predicts the full stationary distribution of population sizes and allele frequencies in different habitats, thus clarifying the conditions under which local adaptation is maintained across habitats under divergent selection, or conversely, those that result in maladaptation and extinction in rare habitats. The underlying approximations (especially, LE) can be formally justified as $r_0 \to 0$ (Fig. 4). Thus, they may not be accurate in typical populations, where growth rates may be high. Similarly, fluctuations in population size are assumed to be only due to demographic stochasticity, and so may be greatly underestimated. Nevertheless, our modeling approach captures key processes involved in local adaptation, and our approximations apply over a broader range. We aim at understanding fundamental processes, rather than precise prediction.

We identify two distinct reasons why local adaptation fails within a rare habitat. First, if selection on locally favored alleles is weak relative to drift, then alleles favored in the common habitat tend to fix across the metapopulation, even when migration is extremely rare, that is, $M \to 0$ (Fig. 5). A somewhat paradoxical consequence of this result is that in the low M limit, loci that are under weak divergent selection across habitats are expected to show *weaker* differentiation than neutral loci, due to a net bias towards alleles favored in the abundant habitat in the former case. In practice, we expect the time scale for loss of divergence at weakly selected loci to increase as $M \to 0$. Thus, local adaptation may be metastable and the loss of polymorphism extremely slow in this regime: this is also observed in individual-based simulations (results not shown).

The loss of local adaptation due to swamping from the abundant habitat, even under weak migration, is not predicted by deterministic arguments, and requires selection (per locus) to be weak relative to drift. This drift-dominated regime also emerges with soft selection, where we obtain an explicit expression for the critical selection threshold required for polymorphism (eq. 5). This threshold depends on the relative proportions of the two habitats: increasingly stringent selection per locus is required to maintain local adaptation in the rare habitat as it becomes more marginal (i.e., ρ decreases; Fig. 2B). Conversely, when the two habitats are equally abundant ($\rho = 1/2$), the critical selection threshold goes to zero as $M \to 0$ (see also Blanquart et al. (2012), who analyze this case with soft selection).

Local adaptation in the rare habitat can fail, even when selection per locus dominates over drift, if migration exceeds a critical threshold. Such thresholds emerge quite generally also with single loci under soft selection that are subject to maladaptive gene flow. In the present model (with hard selection and multiple selected loci), the total migration load sets a more severe constraint: it must be sufficiently low that the population can still grow. Since migration load scales with the number of loci under divergent selection, moderate maladaptation at many loci is sufficient to cause the population to crash. Declining population sizes further reduce the efficacy of selection at individual loci via increased drift but also result in stronger swamping, generating a positive feedback that extinguishes populations in the rare habitat. This feedback sets an upper limit on the migration rate (given L), or alternatively, on the number of loci that can be divergently selected across the two habitats (given M), while still allowing local adaptation in both. Interestingly, we find that the critical level of maladaptive gene flow that populations can withstand actually decreases with increasing selection per locus, if the number of divergently selected loci is large, such that $LS \gtrsim 1$ (Fig. 6). The decrease in local adaptation with increasing intensity of selection, at a given M, was also noted by Ronce and Kirkpatrick (2001) in their deterministic analysis of two habitats under stabilizing selection. However, in the regime where maladaptation leads to extinction, that is, for $LS \gtrsim 1$, critical migration rates are poorly predicted by deterministic analyses (Fig. 6A) which fail to account for the stochastic distribution of population sizes and the risk of extinction (of individual demes) within habitats that are adapted as a whole.

Our analysis thus highlights the difficulty of maintaining more than a few divergently selected alleles across habitats under hard selection, especially when one habitat is rarer. Selection per allele must be sufficiently strong to prevent swamping from the common habitat (even under extremely weak migration), but not so strong that the total fitness cost of maladaptation (due to migration load at multiple divergently selected loci) overwhelms population growth, triggering extinction. Thus, with increasing L, the conditions under which populations in the rare habitat can escape one or the other mode of failure become increasingly restrictive (Figs. 5A and B, and 6B).

Note that in our model, polygenic adaptation is difficult because of the rather extreme form of environmental heterogeneity, in which any selected allele has opposite effects on fitness in the two habitats. In an alternative model, where fitness depends on traits under stabilizing selection toward habitat-specific optima (as in Ronce and Kirkpatrick 2001), migration load would be independent of the number of trait loci in the large L limit (Barton and Etheridge 2018), and would thus not constrain the number of polymorphisms that can be maintained under hard selection. In this case, local adaptation is accomplished via small and transient allele frequency differences at multiple loci.

A key result is that local adaptation in the rare habitat becomes more difficult as selection becomes more "hard" (Fig. 5C): hard selection depresses population sizes, causing both drift and migration to become stronger relative to selection at individual loci. Thus, hard selection and random drift can substantially increase the damage that gene flow may cause, for example, when farmed fish escape into wild populations (Glover et al. 2017).

We focus here on the case where locally adapted populations are demographically stable. However, the joint distribution derived in equation (3) can be used to explore alternative regimes. For instance, we might consider a metapopulation with many very small demes and frequent extinction (i.e., $\zeta = r_0 K \sim 1$). The whole metapopulation can still adapt to *global* selection pressures (if migration is sufficiently high), even when selection within each deme is weaker than local drift. Indeed, Wright (1932) argued that such a "shifting balance" allows efficient search across alternative adaptive peaks (see Rouhani and Barton 1993; Coyne et al. 1997). However, it would not be possible for populations to adapt to local variations in environment between demes in this regime.

The framework presented here is quite general, and applies directly to a wider range of cases, for example, when the metapopulation encompasses more than two habitats or patches with heterogeneous carrying capacities and/or growth rates. While we have focused on local adaptation, the framework can be used to address other questions. For example, the model extends to include dominance, and so could be used to understand how heterosis and inbreeding depression influence local extinctions.

Our analysis neglects LD between locally adaptive alleles, which facilitates simultaneous local adaptation over a wider range of migration rates than predicted by the diffusion (Fig. 4), because sets of introgressing alleles from differently adapted populations are eliminated together, thus reducing the effective rate of gene flow (Barton and Bengtsson 1986). This effect is especially marked in the strong coupling regime (Fig. 4B), where there is a strong positive feedback between a reduction in migration load (due to LD) and an increase in population size. The effects of LD can be incorporated, at least approximately, within the diffusion framework via the heuristic of effective migration rates; we defer analysis to future work. It may also be possible to estimate the extent of local adaptation, and the extent to which it reduces effective gene flow, by observing how divergence and LD vary along the genome (cf. Aeschbacher et al. 2017).

Local adaptation in a metapopulation may lead to parapatric speciation, despite gene flow: as populations diverge, selection against introgressing alleles increases, reducing effective migration, and allowing further divergence. A key issue here is whether a heterogeneous environment will lead to distinct clusters, separated by strong barriers to gene flow, which eventually become good biological species. This may depend on the distribution of available habitats. If these are broadly continuous, and select along multiple environmental dimensions, then there may be substantial local adaptation without clusters being apparent. However, with distinct environments, local adaptation may lead to strong isolation, as multiple divergent loci become coupled together (Barton and De Cara 2009). The framework developed here may be used to investigate how the distribution of selective challenges influences whether populations evolve as generalists, adapting to a range of local environments, or split into distinct and well-isolated species.

AUTHOR CONTRIBUTIONS

E.S. and N.H.B. designed the study; E.S., H.S., and N.H.B. did the mathematical analysis; H.S. did the simulations; E.S., H.S., and N.H.B. wrote the manuscript.

ACKNOWLEDGMENTS

We thank the reviewers for their helpful comments, and also our colleagues, for illuminating discussions over the long gestation of this paper.

CONFLICT OF INTEREST

The authors declare no conflict of interest.

DATA ARCHIVING

Mathematica notebooks (for mathematical and numerical analysis) and Fortran code (for individual-based simulations) are available at https://datadryad.org/stash/dataset/doi:10.5061/dryad.8gtht76p1.

LITERATURE CITED

Aeschbacher, S., J. P. Selby, J. H. Willis, and G. Coop. 2017. Population-genomic inference of the strength and timing of selection against gene flow. Proc. Natl. Acad. Sci. 114:7061–7066.

Banglawala, N. 2010. Local adaptation under demographic and genetic fluctuations. Doctoral diss. The University of Edinburgh, Edinburgh.

Barton, N., and B. O. Bengtsson. 1986. The barrier to genetic exchange between hybridising populations. Heredity 57:357–376.

Barton, N., and A. Etheridge. 2018. Establishment in a new habitat by polygenic adaptation. Theor. Popul. Biol. 122:110–127.

Barton, N. H., and M. A. R. De Cara. 2009. The evolution of strong reproductive isolation. Evolution 63:1171–1190.

Black, A. J., and A. J. McKane. 2012. Stochastic formulation of ecological models and their applications. Trends Ecol. Evol. 27:337–345.

Blanquart, F., S. Gandon, and S. L. Nuismer. 2012. The effects of migration and drift on local adaptation to a heterogeneous environment. J. Evol. Biol. 25:1351–1363.

Carroll, S. P., and C. Boyd. 1992. Host race radiation in the soapberry bug: natural history with the history. Evolution 46:1052–1069.

Chevin, L.-M., O. Cotto, and J. Ashander. 2017. Stochastic evolutionary demography under a fluctuating optimum phenotype. Am. Nat. 190:786–802.

Coyne, J. A., N. H. Barton, and M. Turelli. 1997. Perspective: a critique of Sewall Wright's shifting balance theory of evolution. Evolution 51:643–671.

Dobler, S., and B. Farrell. 1999. Host use evolution in Chrysochus milkweed beetles: evidence from behaviour, population genetics and phylogeny. Mol. Ecol. 8:1297–1307.

Fisher, R. A. 1922. On the mathematical foundations of theoretical statistics. Philos. Trans. R. Soc. Lond. 222:309–368.

———. 1930. The genetical theory of natural selection. Oxford: Clarendon Press.

Glover, K. A., M. F. Solberg, P. McGinnity, K. Hindar, E. Verspoor, M. W. Coulson, M. M. Hansen, H. Araki, Ø. Skaala, and T. Svåsand. 2017. Half a century of genetic interaction between farmed and wild Atlantic salmon: status of knowledge and unanswered questions. Fish Fish. 18:890–927.

Gomulkiewicz, R., and R. D. Holt. 1995. When does evolution by natural selection prevent extinction? Evolution 49:201–207.

Gonzalez, A., O. Ronce, R. Ferriere, and M. E. Hochberg. 2013. Evolutionary rescue: an emerging focus at the intersection between ecology and evolution. Philos. Trans. R. Soc. B 368:20120404.

Govaert, L., E. A. Fronhofer, S. Lion, C. Eizaguirre, D. Bonte, M. Egas, A. P. Hendry, A. De Brito Martins, C. J. Melián, J. A. Raeymaekers, et al. 2019. Eco-evolutionary feedbacks—theoretical models and perspectives. Funct. Ecol. 33:13–30.

Grant, P. R., and B. R. Grant. 2006. Evolution of character displacement in Darwin's finches. Science 313:224–226.

Hanski, I., and T. Mononen. 2011. Eco-evolutionary dynamics of dispersal in spatially heterogeneous environments. Ecol. Lett. 14:1025–1034.

Kawecki, T. J. 2008. Adaptation to marginal habitats. Annu. Rev. Ecol. Evol. Syst. 39:321–342.

Kimura, M. 1955. Solution of a process of random genetic drift with a continuous model. Proc. Natl. Acad. Sci. USA 41:144.

Kinnison, M. T., and A. P. Hendry. 2001. The pace of modern life II: from rates of contemporary microevolution to pattern and process. Genetica 112:145–164.

Kokko, H., and A. López-Sepulcre. 2007. The ecogenetic link between demography and evolution: can we bridge the gap between theory and data? Ecol. Lett. 10:773–782.

Lande, R. 1993. Risks of population extinction from demographic and environmental stochasticity and random catastrophes. Am. Nat. 142:911–927.

Lande, R., S. Engen, and B.-E. Stther. 1998. Extinction times in finite metapopulation models with stochastic local dynamics. Oikos 83:383–389.

Lande, R., S. Engen, and B.-E. Saether. 2003. Stochastic population dynamics in ecology and conservation. Oxford Univ. Press, Oxford.

Lion, S. 2018. Theoretical approaches in evolutionary ecology: environmental feedback as a unifying perspective. Am. Nat. 191:21–44.

Mangel, M., and C. Tier. 1993. Dynamics of metapopulations with demographic stochasticity and environmental catastrophes. Theor. Popul. Biol. 44:1–31.

Ovaskainen, O., and B. Meerson. 2010. Stochastic models of population extinction. Trends Ecol. Evol. 25:643–652.

Polechová, J. 2018. Is the sky the limit? On the expansion threshold of a species' range. PLoS Biol. 16:e2005372.

Polechová, J., and N. H. Barton. 2015. Limits to adaptation along environmental gradients. Proc. Natl. Acad. Sci. 112:6401–6406.

Ronce, O., and M. Kirkpatrick. 2001. When sources become sinks: migrational meltdown in heterogeneous habitats. Evolution 55:1520–1531.

Rouhani, S., and N. Barton. 1993. Group selection and the shifting balance. Genet. Res. 61:127–135.

Sachdeva, H. 2019. Effect of partial selfing and polygenic selection on establishment in a new habitat. Evolution 73:1729–1745.

Thompson, J. N. 1998. Rapid evolution as an ecological process. Trends Ecol. Evol. 13:329–332.

Tufto, J. 2001. Effects of releasing maladapted individuals: a demographic-evolutionary model. Am. Nat. 158:331–340.

Whitlock, M. C., and N. H. Barton. 1997. The effective size of a subdivided population. Genetics 146:427–441.

Wright, S. 1932. The roles of mutation, inbreeding, crossbreeding, and selection in evolution. Proc. 6th Int. Cong. Genet. 1:356–366.

Associate Editor: S. Glemin
Handling Editor: D. Hall

Supporting Information

Additional supporting information may be found online in the Supporting Information section at the end of the article.

Figure S1: Local adaptation in scenarios with asymmetric selection across habitats.

Figure S2: Comparison of individual-based simulations with predictions of the diffusion approximation (eqs. 3 and 4 in the main text).